8. D. E. Okhitsimskii, I. L. Kondrasheva, et al., "Calculation of a point explosion with allowance for counter pressure," Trudy MIAN SSSR, 50, 1 (1957).
9. V. P. Korobeinikov and P. I. Chushkin, "Method of calculating a point explosion in a gas," Dokl. Akad. Nauk SSSR, 154, No. 3 (1964).
10. V. P. Korobienikov and L. V. Shidlovskaya, "A numerical solution for an explosion in a moving gas," in: Numerical Methods in the Mechanics of Continuous Media [in Russian], Vol. 6, No. 4 (1975).
11. E. I. Andriankin, "High-Speed collision of two plates," Zh. Prikl. Mekh. Tekh. Fiz., No. 4 (1963).
12. V. V. Podlubnyi and A. S. Fonarev, "Reflection of a spherical wave from a flat surface," Izv. Akad. Nauk SSSR, Mekh. Zhid. Gaza, No. 6 (1974).
13. É. I. Andriankin, "Effects of radiative conduction on the gas flow in a strong explosion," Inzh.-Fiz. Zh., 4, No. 11 (1961).
14. É. I. Andriankin, "Propagation of a non-selfmodeling heat wave," Zh. Eksp. Teor. Fiz., 35, No. 2 (8) (1958).
15. Ya. B. Zel'dovich and Yu. P. Raizer, Physics of Shock Waves and High-Temperature Hydrodynamic Phenomena [in Russian], Fizmatgiz, Moscow (1963).

INVESTIGATION OF THE SHOCK COMPRESSION OF LIQUID TIN AT PRESSURES UP TO 100 GPa AND INITIAL TEMPERATURES OF 310...475°C

K. V. Volkov and V. A. Sibilev

UDC 536.242:546.3

The melting of materials when subjected to shock compression and the equation of state of the liquid phase has been considered in [1-4]. Numerous experimental results on the dynamic compressibility of different materials up to 1 TPa, e.g., [5-7], show that melting in a shock wave is only slightly affected by the variation of the shock adiabatic curve in p–U and p–V coordinates (p is the pressure, U is the mass velocity, and V is the specific volume). The experimental data up to pressures of 0.1-0.15 TPa are well described by a linear D–U relationship. At higher pressures there is a reduction in the slope of the D–U curve, due to melting in the shock wave [3], and the D–U curve in the liquid-phase region takes the form of a straight line but with a smaller slope than for the solid phase. However, it should be noted that from the existing experimental points one could equally successfully draw a D–U curve with a gradually reducing slope. Such attempts have been made (see, e.g., [8]). On the other hand, it was pointed out in [3] that a gradual reduction in the slope of the D–U curve may be due to an increase in the contribution of the electron component in the equation of state at high temperatures. Hence, it is difficult to draw any definite conclusions regarding the effect of melting on the form of the D–U curve. Information on this can, in principle, be obtained if one has experimental D–U curves of the initially solid and initially liquid phases. We know of only one publication in which shock compression of a liquid metal (mercury) has been investigated [9]. As far as we are aware no comparative data on the shock loading of an initially liquid and an initially solid phase of metals exists.

1. Calculation of the Shock Adiabatic Curves of Al and Cu and an Estimate of the Shock Adiabatic Curves of Liquid Sn. Using the semi-empirical equations of state proposed in [3] we calculated the shock adiabatic curves of the initially solid and liquid phases of Al and Cu. The initial state of the liquid phases was taken at t = 2000°C for Al ($\rho_{0l} \approx 2.1$ g/cm^3, and $E_{0l} \approx 217 \cdot 10^8$ erg/g) and at t = 2500°C for Cu ($\rho_{0l} \approx 7.1$ g/cm^3 and $E_{0l} \approx 142 \cdot 10^8$ erg/g). Considerable overheating above the melting point was then taken in order to explain the difference in the behavior of the shock adiabatic curves of the solid and liquid phases and particularly the slope of the D–U curves. We also carried out calculations using the equation of state of the liquid phase for the initially solid state of Al and Cu (Table 1).

In Fig. 1 (in the same coordinates as in [3]) we plot curves for Al (curve 1 is experimental [10], curve 2 is calculated for the solid phase, curve 3 is calculated for the liquid phase with ρ_{0l}, E_{0l}, curve 4 is calculated for the liquid phase with ρ_{0s}, E_{0s}, and curve 5 is

Translated from Zhurnal Prikladnoi Mekhaniki i Tekhnicheskoi Fiziki, No. 4, pp. 125-132, July-August, 1981. Original article submitted June 4, 1980.

0021-8944/81/2204-0551$07.50

TABLE 1

	ρ, g/cm^3	$p\cdot10^{-1}$, TPa	$D\cdot10^{-6}$, cm/sec	$U\cdot10^{-6}$, cm/sec	$E\cdot10^{-10}$, erg/g	$T\cdot10^{-3}$, K
Shock adiabatic curve of solid Al	3,208	0,187	0,678	0,101	0,351	0,298
	3,822	0,612	0,886	0,253	3,044	1,388
	4,368	1,260	1,109	0,416	8,494	4,276
	4,914	2,254	1,363	0,606	18,190	9,664
	5,460	3,679	1,642	0,821	33,536	17,658
	6,000	5,603	1,941	1,058	55,772	28,003
Shock adiabatic curve of liquid Al with ρ_{0l}, and E_{0l}	2,866	0,232	0,643	0,172	3,648	3,354
	3,344	0,576	0,859	0,320	7,276	6,022
	4,095	1,589	1,246	0,607	20,607	14,601
	4,368	2,140	1,401	0,727	28,628	19,191
	4,914	3,613	1,733	0,993	51,438	30,701
	5,187	4,574	1,913	1,138	66,982	37,633
Shock adiabatic curve of liquid Al with ρ_{0s} and E_{0s}	4,368	1,289	1,122	0,421	9,014	3,467
	4,914	2,277	1,370	0,609	18,690	9,078
	5,460	3,647	1,634	0,817	33,555	17,262
	6,000	5,439	1,912	1,042	54,452	27,577
Shock adiabatic curve of solid copper	10,977	0,494	0,548	0,101	0,432	0,557
	12,571	1,264	0,701	0,201	1,951	2,248
	13,890	2,339	0,858	0,304	4,557	5,880
	16,058	5,475	1,176	0,520	13,429	18,916
	17,473	8,773	1,418	0,691	23,778	32,912
Shock adiabatic curve of liquid copper with ρ_{0l} and E_{0l}	10,977	1,137	0,673	0,238	4,247	10,411
	12,571	2,360	0,874	0,380	8,654	18,913
	13,890	3,917	1,062	0,519	14,906	29,710
	15,525	6,743	1,323	0,718	27,190	47,946
Shock adiabatic curve of liquid copper with ρ_{0s} and E_{0s}	13,266	1,785	0,783	0,254	3,808	3,231
	15,002	3,612	1,000	0,403	8,193	11,643
	16,551	6,062	1,214	0,557	15,590	24,006
	17,918	8,976	1,416	0,708	25,118	38,274

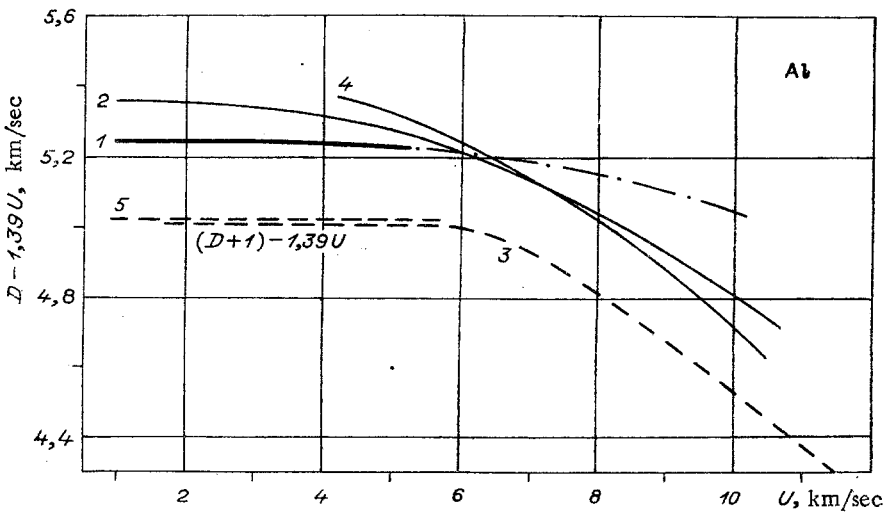

Fig. 1

the approximate estimate for the initially liquid phase, see below). Note that curve 4 coincides with the similar curves taken from [3], whereas the curve for the solid phase 2 has a quite different form (the "overheated" solid phase from [3] is shown by the dash–dot curve).

It follows from the calculations that the D–U curves for the initially liquid phase of Al and Cu are only shifted with respect to the D–U curves for the initially liquid phase, and repeat their shape. Their slopes are the same over the whole pressure range, and the reduction in the slope as the pressure increases appears to an equal extent for both phases.

Data from the equation of state of liquid Sn are not available in [3], so its shock adiabatic curve was obtained from the shock adiabatic curve of the solid phase using the following simple estimates, the applicability of which was checked by comparison with the accurate calculations for Al given above.

We can consider the solid and liquid phases as independent materials each with its own initial density ρ_0 and initial velocity of sound $c_0 = \left(\frac{\partial p}{\partial \rho}\right)_S^{1/2}$, and we can use the equation of the shock adiabatic curve, for example the well-known equation with the limiting density [11]

$$p(\sigma) = \frac{\rho_0 c_0^2}{n} \frac{\sigma^n \left(h - \frac{n+1}{n-1}\right) + \sigma \frac{2n}{n-1} - (h+1)}{h - k\sigma}, \tag{1.1}$$

taking n and h to a first approximation to be the same for both phases (k = 1). For the same compression σ, taking the laws of conservation into account, we have the following relations between the parameters of the initially solid and liquid phases:

$$p_l \simeq \frac{\rho_{0l}}{\rho_{0s}} \frac{c_{0l}^2}{c_{0s}^2} p_s, \quad D_l \simeq \frac{c_{0l}}{c_{0s}} D_s, \quad U_l \simeq \frac{c_{0l}}{c_{0s}} U_s. \tag{1.2}$$

In Fig. 1 curve 5 corresponds to the approximate estimate considered using relations (1.2). The values of the initial densities and the initial velocities of sound for Al (ρ_{0S} = 2.73 g/cm³, $\rho_{0l} \approx$ 2.1 g/cm³, c_{0S} = 5.34 km/sec [8], and c_{0l} = 4.28 km/sec [12]) are taken at a temperature of 2000°C.

It can be seen that the estimate of the shock adiabatic curve of the initial liquid Al obtained in this way is in good agreement with the value calculated above using the semi-empirical equation of state of the liquid phase.

Taking for Sn, ρ_{0S} = 7.28 g/cm³, ρ_{0l} = g/cm³, c_{0S} = 2.67 km/sec [8], and c_{0l} = 2.44 km/sec [13] (ρ_{0l} and c_{0l} are taken at t = 410°C, which corresponded to the temperature in the experiments with liquid tin), we obtain for the same compression

$$p_l = 0.789 p_s, \; D_l = 0.914 D_s, \; U_l = 0.914 U_s. \tag{1.3}$$

The shock adiabatic curve of liquid tin constructed from these relations is shown by the broken curve in Fig. 2. For estimates and comparisons at pressures of around 10 GPa we used extrapolation of the D–U relation obtained in the pressure range 17-42 GPa, D = 2.38 + 1.712U [8], and at higher pressures the shock adiabatic curve from [5] (the continuous curve with the experimental points in Fig. 2).

2. Determination of the Points of the Shock Adiabatic Curve of Liquid Tin. For the investigations we chose tin, which possesses less physicochemical activity, is less liable to oxidize when heated, and is less toxic than other easily fusible metals. In Fig. 3 we show the phase diagram of tin [14] (1 is the melting curve, and 2 is the calculated shock adiabatic curve of solid tin [6]). The conventional shock-adiabatic curves of liquid tin 3 were obtained by parallel transfer of the shock adiabatic curves of solid tin (the expected breaks on intersecting the melting curve are not shown). The shock adiabatic curve touches the melting curve at the initial temperature of ∿400°C.

Three points of the shock adiabatic curve of liquid tin were obtained from the initial temperature of 410°C at pressures of 9, 68.5, and 82.5 GPa from measurements of the velocity of the shock wave using the reflection method [15]. We also carried out experiments with solid tin in a similar reaction for direct comparison of the results.

The pressure in the specimen of ∿10 GPa was produced by the impact of an aluminum piston of diameter 65 mm accelerated by a gunpowder gun. The column was arranged vertically, the measuring unit was placed in the nozzle, and the air from the channel of the column was pumped out by a fore vacuum pump. The velocity of the piston (1 km/sec) was measured in separate experiments. The mean square spread of the series of 4-6 experiments was not more than 20 m/sec. The pressure in the specimen of 68.5 and 82.5 GPa was produced by the impact

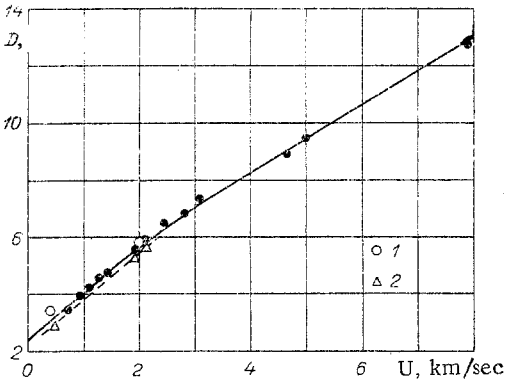

Fig. 2

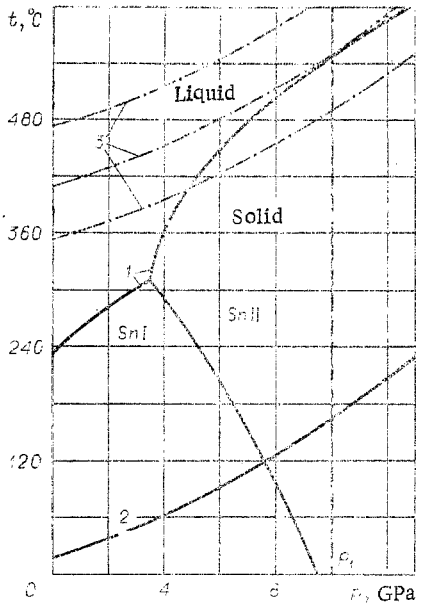

Fig. 3

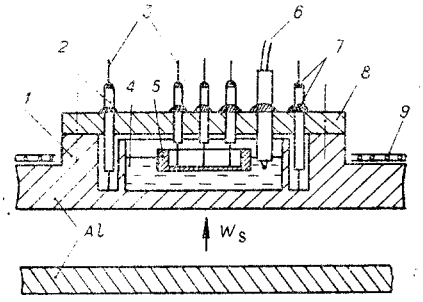

Fig. 4

of aluminum plates accelerated by an explosion. The striker of thickness 8 mm had a flight velocity of 4.66 km/sec, and the one of thickness 2 mm had a flight velocity of 5.21 km/sec. We used an electrical contact method of measurement employing an electric spark equipment and spectrophotometer recording.

The arrangement used in the experiments to measure the velocity of the shock wave in liquid tin is shown in Fig. 4. The screen-container 1 for the tin 4 is made of aluminum coated with a specially thickened oxide film (50-100 μm) by anodizing. The oxide film protects the aluminum from the aggressive action of the melted tin and serves as electrical insulation for the electrical contacts 3. The electrical contacts at the upper level (5...8 pieces) rests in the anodized bottom of the "float" 5, and the contacts of the lower level (8 pieces) rest in the bottom of the ring hollow of the container. When calculating the velocity of the shock wave in the melt we introduced a correction for the thickness of the bottom of the float (0.25 mm). The heater was a plane nichrome helix in asbestos insulation 9, placed on the screen-container. The temperature of the melt was measured with a chromel–copel thermocouple 6. The electrical contacts and the thermocouple were insulated from the metal panel 8 with steatite tubes 2, which were fastened with thermally stable cement 7 based on liquid glass and talc. When assembling the measuring system the cement was thermally processed. The measuring unit was then cooled. When carrying out the experiment the measuring system was heated (experiments with solid tin were carried out without heating).

The results of the experiments are shown in Table 2 and represented in Fig. 2 (1 is solid tin and 2 is liquid tin). When processing the data of the reflection method [15] for low pressures we used the experimental shock adiabatic curve of aluminum obtained in the pressure range from 4 GPa to 21 GPa [16] (the screen-container and the striker in this case were made of D16 aluminum alloy). At high pressures (AMTs aluminum alloy was employed) we

TABLE 2

Striker velocity W_s, km/sec	Aggregate state	Initial temperature, °C	Measurement base, Δ, mm	Number of experiments	$\bar{D}$, km/sec	$s_{\bar{D}}$, km/sec	p, GPa	U, km/sec
1,0	Liquid	410	4	4	2,89	0,08	9,1	0,46
	Solid	20	4	3	3,43	0,06	10,0	0,41
4,66	Liquid	410	10	4	5,40	0,03	68,5	1,86
5,21	Liquid	410	4	4	5,79	0,06	82,5	2,08
	Solid	20	4	2	5,80	0,12	85,0	2,02

used the D–U relation D = 5.25 + 1.39U as in [3, 10].

We checked the effect of initial heating of the aluminum on its properties for shock compression by measuring the velocity of the shock wave in the aluminum screen heated to 410°C, and also when unheated for direct comparison, for a striker velocity of 5.21 km/sec. The velocities (8.87 for the heated screen and 8.92 km/sec for the cold screen) agree within the limits of experimental error (~1%). This agrees with the data obtained in [17] for brass.

For a striker velocity of 1 km/sec the velocity of the shock wave in the solid tin, according to the shock adiabatic curve, extrapolated from the D–U relation from the 17-42 GPa region should be D'_s = 3.04 km/sec. It can be assumed that within the limits of error $D_l = D'_s$. However, the measured velocity in solid tin (3.43 km/sec) is much higher. At high pressures the measured velocities and the solid and liquid tin are practically identical for the same striker velocity, and the results for liquid tin agree quite well with the shock adiabatic curve estimated from relations (1.3).

3. Crystallization of Tin in the Shock Wave. At initial temperatures of the liquid tin of less than 400°C its shock adiabatic curve intersects the melting curve (see Fig. 2) and it is possible for the liquid tin to solidify when shock loaded. The question of the shock compression of a material with a phase transition and an increase in density is considered in [15]. If there is no supercooling of the liquid tin in the shock wave and its crystallizes, it should manifest itself in a change in the mass velocity. If the initial temperature of the liquid tin is reduced, then on passing through the limiting temperature of 400°C we would expect an increase in the free surface velocity (for a constant velocity of the striker).

The arrangement used to measure the free-surface velocity of the tin melt is shown in Fig. 5. The screen-container 1 of anodized aluminum is heated with a nichrome spiral in asbestos insulation 2. The temperature of the tin melt 3 was measured with a chromel–copel thermocouple 4. According to existing data, the free surface of the liquid when the shock wave reaches it moves irregularly and forms drops. In addition, in our case oxides are formed on the surface of the liquid tin which hinders the measurements. We used a titanium indicator 5, 0.4 mm thick, which was immersed in the melt. Titanium is unaffected by the agressive action of the liquid tin and the shock adiabatic curves of titanium and tin are very close in p–U coordinates, and over the working pressure range titanium is somewhat "harder" than tin and hence does not break away from its surface after the shock wave emerges into the air. The distance at which acceleration of the titanium layer up to the velocity of the free surface of the liquid tin occurs, according to estimates, is less than 0.5 mm.

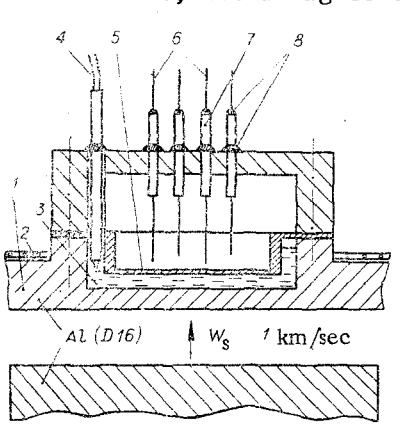

Fig. 5

TABLE 3

t_{in}, °C	W_i, m/sec	S_i, m/sec	$\frac{S_i}{W_i}100$, %	t_{in}, °C	W_i, m/sec	S_i, m/sec	$\frac{S_i}{W_i}100$, %
475	877	14	1,6	380	916	29	3,2
440	878	16	1,8	375	914	30	3,3
410	884	24	2,7	370	899	23	2,6
405	883	16	1,8	355	921	33	3,6
400	904	18	2,0	340	955	30	3,2
390	955	26	2,7	310	897	20	2,2

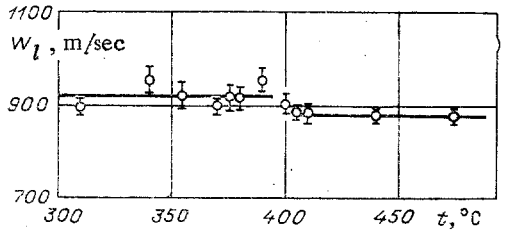

Fig. 6

Over the indicator we placed 16 electrical contacts 6 in staggered order in the form of copper wires 0.5 mm in diameter in steatite tubes 7, fixed with heat resisting cement 8. The lower level was 0.5 mm from the indicator. The base of the measurement was 2-2.5 mm, and the thickness of the layer of liquid tin under the indicator was 4 mm. The results of the measurements are shown in Table 3 and are plotted in Fig. 6. It can be seen that the measurement error and the spread in the values of the velocity themselves is greater for t < 400°C, which may be due to the fact that crystallization and the reverse transition into the liquid state after overloading gives rise to nonplanarity of the titanium indicator on the surface of the tin. The results of the measurements, like those at 400°C, show jumps in the $W_l(t)$ curve. Unfortunately, it is not possible from the existing experimental data to be able to say with sufficient reliability what sort of curve the experimental points describe — a double-step (as shown in Fig. 6) or a single inclined straight line, since the difference in the variances of these relations is negligible [18].

4. Analysis of the Results. When the pressure in the shock wave is increased the difference between the specific volumes [19] and the velocities of sound [2] between the solid and liquid phases decrease to the value of the experimental error, i.e., the liquid phase approaches the solid phase in its properties, at least in the region of the melting curve. The method of determining the melting point by the shock compression of porous materials proposed in [20], based on theoretical estimates (from the existing semi-empirical equations of state) of the variation in the velocity of the shock wave on melting could not be confirmed experimentally.

The results we obtained from measurements of the shock-wave velocity in the initially solid and liquid tin showed that for the same state in the screen (a screen of Al) the difference in the velocities lies within the limits of experimental error (1-2%). The difference in the shock-wave velocities obtained at low pressures (~10 GPa) may be connected with the elastic sign in solid tin or due to splitting of the shock wave due to the phase transition of tin (SnI) into a denser modification (SnII, see Fig. 2). When the pressure is increased we would obviously expect the appearance of a greater tendency to approach the values of the shock-wave velocity for the initially solid and liquid phases for the same state in the screen even for considerable overheating above the melting point. Experimental data for porous metals [1, 21] indicates this to some extent. A change in the porosity over a wide range (from 1 to 4) has a small effect (a few percent) on the shock-wave velocity particularly when the pressure is increased. If the shock-wave velocity in the melt and the initially solid phase are equal (the state in the screen is the same), the shift of the shock adiabatic curve of the initially liquid phase with respect to the shock adiabatic curve of the solid phase when constructing the experimental points using the p—U diagram method is due exclusively to the reduction in the initial density. Calculations and estimates carried out for Al, Cu and Sn in section 1 indicate that for the initially liquid phase the slope of the D—U curve is not less than for the initially solid phase. The experimental data obtained for

liquid tin also indicate this. The smooth drop in the slope of the D–U curves as the pressure in the shock wave increases is most likely due to an increase in the contribution of the electron component in the equation of state.

In [22] a generalized shock adiabatic curve of materials was proposed in the form

$$p_i\left(\frac{V}{V_0}\right)=\frac{\rho_{0i}}{\rho_{0j}}\frac{k_j^2}{k_i^2}p_j\left(\frac{V}{V_0}\right),\quad D_i\left(\frac{V}{V_0}\right)=\frac{k_j}{k_i}D_j\left(\frac{V}{V_0}\right),\quad U_i\left(\frac{V}{V_0}\right)=\frac{k_j}{k_i}U_j\left(\frac{V}{V_0}\right),$$

where k_i and k_j are certain constants which refer to different materials. This is practically approximation (1.2) of the present paper, only the constants k_i and k_j in (1.2), unlike [22], are defined and have the meaning of the inverse velocity of sound determined by the compressibility of the material. Although the results obtained in [22] have a generalized statistical character they once again confirm that to a first approximation the shock compressibility of materials is determined by their acoustic rigidity.

We can say from the results of measurements of the free-surface velocity of the tin melt at different initial temperatures that a phase transition of the liquid tin into the solid phase has occurred and vice versa when it is loaded up to GPa at initial temperatures of <400°C.

LITERATURE CITED

1. S. B. Kormer et al., "Dynamic compression of porous metals and the equation of state with variable heat capacity at high temperatures," Zh. Eksp. Teor. Fiz. 42, No. 3 (1962).
2. V. D. Urlin and A. A. Ivanov, "Melting during shock-wave compression," Dokl. Akad. Nauk, SSSR, 149, No. 6 (1963).
3. V. D. Urlin, "Melting at very high pressures obtained in a shock wave," Zh. Eksp. Teor. Fiz. 49, No. 2(8) (1965).
4. L. V. Al'tshuler et al., "Overloading isentropy and the equation of state of metals at high energy densities," Zh. Eksp. Teor. Fiz. 78, No. 2 (1980).
5. L. V. Al'tshuler, A. A. Bakanova, and R. F. Trunin, "Shock adiabatic curves and zero isotherms of seven metals at high pressures," Zh. Eksp. Teor. Fiz., 42, No. 1 (1962).
6. R. G. McQueen and S. P. Marsh, "Equation of state for nineteen metallic elements from shock-wave measurement to two megabars," J. Appl. Phys. 31, No. 7 (1960).
7. S. B. Kormer et al., "Investigation of the compressibility of five ionic compounds up to pressures of 5 Mbar," Zh. Eksp. Teor. Fiz. 47, No. 4(10) (1964).
8. M. Van Thiel, A. S. Kusubov, A. C. Mitchell, and V. W. Davis, Compendium of Shock-Wave Data. Lawrence Radiation Laboratory, University of California, Livermore, UCRL-50108 (1966).
9. J. M. Walsh and M. H. Rice, "Dynamic compression of liquids from measurements on strong shock waves," J. Chem. Phys., 26, No. 4 (1957).
10. L. V. Al'tshuler et al., "Equation of state of aluminum, copper and lead at high pressures," Zh. Eksp. Teor. Fiz. 38, No. 3 (1960).
11. I. P. Dudoladov et al., "Shock compressibility of polystyrene with different initial density," Zh. Prikl. Mekh. Tekh. Fiz. No. 4 (1969).
12. L. D. Kruglov, "The velocity of sound, compressibility, and Gruneisen parameter of Al, Mg, Zn, Sn, Sb and Cd melts," Zh. Fiz. Khim. 50, No. 10 (1976).
13. B. M. Gitis and I. G. Mikhailov, "The velocity of sound and compressibility of certain liquid metals," Akust. Zh. 11, No. 4 (1965).
14. S. E. Babb Jr., "Parameters in the Simon equation relating pressure and melting temperature," Rev. Modern Phys. 35, No. 2 (1963).
15. Ya. B. Zel'dovich and Yu. P. Raizer, The Physics of Shock Waves and High-Temperature Hydrodynamic Phenomena [in Russian], Nauka, Moscow (1966).
16. S. Katz, D. G. Doran, and D. R. Curran, "Hugoniot equation of state of aluminum and steel from oblique shock measurement," J. Appl. Phys. 30, No. 4 (1959).
17. A. C. Mitchell and M. van Thiel, "Effect of temperature on shock-wave propagation in Cu–Zn alloys," J. Appl. Phys. 45, No. 9 (1974).
18. E. I. Pustyl'nik, Statistical Methods of Analyzing and Processing Observations [in Russian], Nauka, Moscow (1968).
19. S. B. Kormer et al., "Experimental determination of the temperatures of shock-compressed NaCl and KCl and their melting curves up to pressures of 700 kbar," Zh. Eksp. Teor. Fiz. 48, No. 4 (1965).

20. A. I. Funtikov, "A method of studying phase transitions at high pressures using shock compression of porous materials," FGV, 5, No. 4 (1969).
21. K. K. Krupnikov, M. I. Brazhnik, and V. P. Krupnikova, "Shock compression of porous tungsten," Zh. Eksp. Teor. Fiz. 42, No. 3 (1962).
22. V. F. Anisichkin, "Generalized shock adiabatic curves of elements," Zh. Prikl. Mekh. Tekh. Fiz. No. 3 (1978).

RESISTANCE OF ALUMINUM AD-1 AND DURALUMINUM D-16 TO PLASTIC DEFORMATION UNDER SHOCK COMPRESSION CONDITIONS

A. N. Dremin, G. I. Kanel', and O. B. Chernikova

UDC 532.593

It is known that the strength properties of a material affect the nature of the evolution and the damping rate therein of shocks of tens of gigapascals in amplitude sufficiently substantially [1-3]. Recording of the evolution of a one-dimensional compression pulse permits determination of the trajectories of the change in state of fixed specimen particles in the coordinates: stress σ_x in the compression direction-specific volume V [4]. Then from the divergence between the trajectories of the change in state and the multilateral compression curve p(V) (for instance, the equilibrium isentropy), by taking account of the one-dimensionality of the total deformation, a law for the variation of the shear stress during deformation can be found and the resistance to deformation can thereby be determined at different stages of compression pulse passage through the specimen particle being checked. Such measurements are performed in this paper for technical aluminum AD-1 with the density 2.71 g/cm³ and duraluminum D-16 with the density 2.78 g/cm³ for two compression pulse amplitudes.

The diagram for the tests is shown in Fig. 1. A one-dimensional compression pulse of initially rectangular shape is generated in the specimen 1 by the impact of an aluminum plate (impactor) 2 accelerated by using an explosive apparatus. Two series of tests are executed, in the first of which the impactor thickness is δ = 5 mm and its velocity is W = 595 ± 10 m/sec. and in the second δ = 4 mm, and W = 1505 ± 20 m/sec. The diameter of the flat section of the impactor was 55-65 mm at the time of collision. The compression pulse was recorded by using manganin pressure transducers 3 located 4-15 mm from the collision surface in the specimens. The specimen plates were fabricated from 120-mm diameter circular billets in the delivered state. The transducers had the area ∿5 × 5 mm, the thickness 0.03 mm, and initial resistance ∿3.5 Ω, and were separated from the specimen surface by 0.02-mm thick (in the first series) or 0.04-mm thick (in the second series) insulating lavsan films 4 on both sides. During the multiple reflections, the pressure in the low-strength insulation is set equal to the normal stress in the compression direction σ_x. Here and henceforth we shall take the compressive stress positive. The stress profiles $\sigma_x(t)$ for aluminum obtained from processing experimental data, are presented in Fig. 2; the stress profiles $\sigma_x(t)$ for duraluminum differ insignificantly. The distance from the collision surface to the transducer is shown in millimeters by the number on the curves. Each curve is obtained by taking the average of the results of at least two measurements, where the hysteresis in the readings of the manganin pressure transducers [5] was taken into account in the processing. According to the test conditions, the rear impactor surface in the second series was in contact with paraffin, consequently, the unloading was not traced completely in these tests.

The elastic part of the rarefaction wave is isolated sufficiently clearly on the pressure profiles. The transition from elastic to plastic waves is smooth and blurred. The tightened "tail" of the rarefaction wave is fixed in the first series of tests. The elastic predecessor of the compression was not determined clearly by the manganin transucers in either the aluminum or the duraluminum case. The characteristic time for shock front growth was ∿0.08-0.11 μsec on the oscillograms for the first test series, and ∿0.05-0.08 μsec for the second test series.

Chernogolovka. Translated from Zhurnal Prikladnoi Mekhaniki i Tekhnicheskoi Fiziki, No. 4, pp. 132-138, July-August, 1981. Original article submitted May 30, 1980.

 0021-8944/81/2204-0558$07.50